Continental Shelf Research 154 (2018) 26–36

Contents lists available at ScienceDirect

Continental Shelf Research

journal homepage: www.elsevier.com/locate/csr

Wave transport in the South Australian Basin

John A.T. Bye[a,b,*], Charles James[a]

[a] SARDI Aquatic Sciences Centre, South Australia, Australia
[b] School of Earth Sciences, The University of Melbourne, Victoria, Australia

ARTICLE INFO

Keywords:
South Australian Basin
Southern Shelf
Wave transport
Stokes velocity
Ekman transport
ROMS simulation

ABSTRACT

The specification of the dynamics of the air-sea boundary layer is of fundamental importance to oceanography. There is a voluminous literature on the subject, however a strong link between the velocity profile due to waves and that due to turbulent processes in the wave boundary layer does not appear to have been established. Here we specify the velocity profile due to the wave field using the Toba spectrum, and the velocity profile due to turbulence at the sea surface by the net effect of slip and wave breaking in which slip is the dominant process. Under this specification, the inertial coupling of the two fluids for a constant viscosity Ekman layer yields two independent estimates for the frictional parameter (which is a function of the 10 m drag coefficient and the peak wave period) of the coupled system, one of which is due to the surface Ekman current and the other to the peak wave period. We show that the median values of these two estimates, evaluated from a ROMS simulation over the period 2011–2012 at a station on the Southern Shelf in the South Australian Basin, are similar in strong support of the air-sea boundary layer model. On integrating over the planetary boundary layer we obtain the Ekman transport ($\frac{w_*^2}{f}$) and the wave transport due to a truncated Toba spectrum ($\frac{w_* z_B}{\kappa}$) where w_* is the friction velocity in water, f is the Coriolis parameter, κ is von Karman's constant and $z_B = \frac{gT^2}{8\pi^2}$ is the depth of wave influence in which g is the acceleration of gravity and T is the peak wave period. A comparison of daily estimates shows that the wave transports from the truncated Toba spectrum and from the SWAN spectral model are highly correlated (r = 0.82) and that on average the Toba estimates are about 86% of the SWAN estimates due to the omission of low frequency tails of the spectra, although for wave transports less than about 0.5 $m^2 s^{-1}$ the estimates are almost equal. In the South Australian Basin the Toba wave transport is on average about 42% of the Ekman transport.

1. Introduction

The Ekman layer is a fundamental feature of the ocean circulation. It is often not realized that its theoretical formulation does not take any account of the existence of the ocean wave field. The basic concept is the existence of an eddy viscosity which takes account of turbulent processes only.

Here we implement a formulation of wave dynamics to complement the original formulation of the turbulent processes given in Ekman (1905), and for clarity we will refer to that part of the coupled boundary layer in which wave motion is dominant as the wave boundary layer, which can be regarded as a sublayer of the planetary boundary layer (Fig. 1). The theoretical results follow from an application of a similarity model which is characterised by approximately logarithmic velocity profiles in the air and the water over the extent of the wave boundary layer. (Bye and Wolff, 2008; Bye et al., 2010). The logarithmic profile in the water including the low and high wave number limits is due to the particle motions of the wave field, and is quite independent of the logarithmic profile in the air which is due to the turbulent motions.

The similarity model has been applied previously to successfully predict the surface drift current (u_s) in the surface drift layer (Fig. 1) and also the mean current in the surface drift layer/wave boundary layers measured by HF Radar (Bye et al., 2017). It has also been applied in the wave boundary layer of the atmosphere (Fig. 1) to predict the 10 m drag coefficient (Bye et al., 2014) in excellent agreement with the consolidated sets of observational data summarized in Foreman and Emeis (2010) and Andreas et al. (2012).

Here, as in the previous studies, we assume a unimodal wave spectrum in which a unique peak wave number can be identified. Thus there are two variables in the similarity model; the wind speed and the peak wave period. The theory relevant to the present study is presented in Section 2, where in particular the two components of current in the wave boundary layer: the Stokes velocity due to the wave field and the

* Corresponding author at: School of Earth Sciences, The University of Melbourne, Victoria, Australia.
E-mail address: jbye@unimelb.edu.au (J.A.T. Bye).

https://doi.org/10.1016/j.csr.2017.12.010
Received 7 July 2017; Received in revised form 1 December 2017; Accepted 21 December 2017

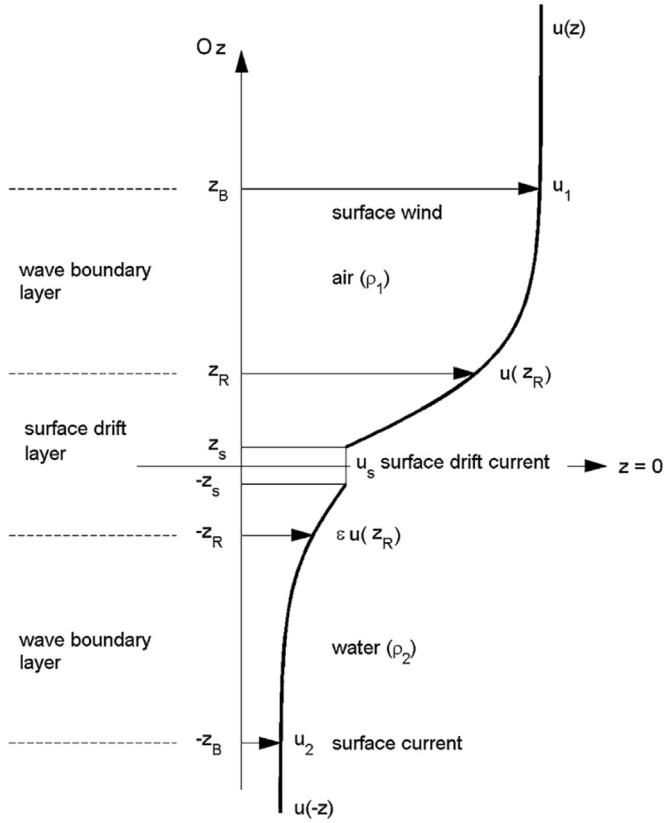

Fig. 1. The velocity structure in the wave boundary layer adapted from Fig. 1 of Bye and Wolff (2008).

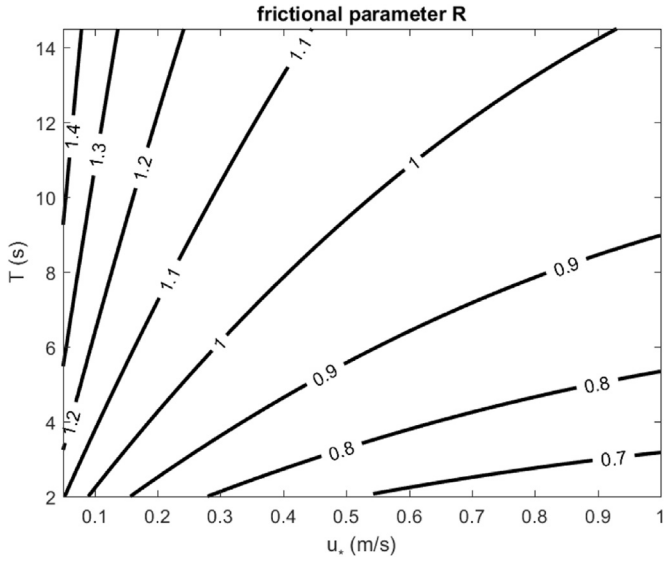

Fig. 2. The frictional parameter (R) as a function of u_* and T, evaluated from equation (A1) in the Appendix of Bye et al. (2014) with $K_{10} = 0.002$ and $u_{10} = 40\ \mathrm{ms}^{-1}$.

turbulent velocity due to wave breaking and slip are identified.

The observational campaign, which was carried out in the South Australian Basin, relied on the implementation of the Regional Ocean Modelling System (ROMS), which incorporates the Simulating Waves Nearshore (SWAN) spectral model, and in which surface forcing, in particular for the wind stress, is from the European Centre Medium Weather Forecasting (ECMWF) archive (Section 3). A detailed comparison between observations and theory is given in Section 4. In Section 5, the importance of the wave transport as a component of the total surface transport in the South Australian Basin is demonstrated for monthly average fields, and Section 6 is a general conclusion in which the relation of the study to other work is discussed.

2. Theory

The velocity profile in the wave boundary layer relative to the surface geostrophic velocity, for a surface shear stress (τ_s) along ox, is,

$$u(-z) = (u_{St}(-z) + u_2, v_2) \tag{1}$$

where oz is vertically upwards from the undisturbed interface ($z = 0$) and $u_{St}(-z)$ is the Stokes velocity due to the irrotational particle motions, u_2 is the turbulent velocity along ox due to slip and wave breaking at the sea surface (Bye et al., 2017), and v_2 is the turbulent velocity along oy. On evaluating the Stokes velocity due to the Toba spectrum (Toba, 1973) bounded by the low (k_0) and high wavenumber (k_1) limits of the wave spectrum, we obtain the logarithmic velocity profile,

$$u_{St}(-z) = \frac{w_*}{\kappa}\ln\frac{z_B}{z}, \quad z_R < z < z_B \tag{2}$$

in which $w_* = \sqrt{\frac{\tau_s}{\rho}}$ is the friction velocity in water where ρ is the water density, $\kappa = 0.4$ is von Karman's constant, and $z_B = \frac{1}{2k_0}$ and $z_R = \frac{1}{2k_1}$ where $\frac{z_R}{z_B} \ll 1$ and $k_0 = \frac{4\pi^2}{gT^2}$ in which T is the peak wave period and g is the acceleration of gravity (Bye, 1988). In (2), $u_{St}(-z_B) = 0$ where on substituting for k_0, $z_B = \frac{gT^2}{8\pi^2}$ is the depth of the wave boundary layer over which the wave motion is significant. On integrating (2) over the depth range ($z_R < z < z_B$) we obtain the wave transport as estimated by the Stokes transport ($\frac{w_* z_B}{\kappa}$) due to the truncated Toba spectrum.

In the water, the drag law is,

$$w_* = \sqrt{K(-z)}\,(u(-z_R) - u(-z)) \tag{3}$$

and in the air, the drag law is,

$$u_* = \sqrt{K(z)}\,(u(z) - u(z_R)) \tag{4}$$

where $u(-z_R)$ which is due to the particle velocities in the water, and which is due to the phase velocities in the air, are the wave induced velocities at the inner edge of the wave boundary layer, and $u_* = \frac{w_*}{\varepsilon}$ in which $\varepsilon = \sqrt{\frac{\rho_a}{\rho}}$ is the friction velocity in air. $K(-z)$ and $K(z)$ are respectively the drag coefficients in water and air.

In the similarity model of the wave boundary layer, aerodynamically rough conditions are assumed to occur, and hence the two drag coefficients are equal, $K(-z) = K(z)$, and also the wave induced velocities at the inner edge of the wave boundary layer are in the ratio,

$$u(-z_R) = \varepsilon u(z_R) \tag{5}$$

Hence from (3) and (4), the drag coefficient at the edge of the wave boundary layer,

$$K(|z_B|) = \left(\frac{\kappa}{\ln\frac{k_1}{k_0}}\right)^2 \tag{6}$$

is determined by the wavenumber extent of the wave spectrum, $k_1 > k > k_0$ (Bye et al., 2017). Further, on eliminating between (3) and (4) using (5), we obtain at $|z| = z_B$,

$$u_2 = \varepsilon u_1 - \frac{w_*}{\sqrt{K_I}} \tag{7}$$

where $u_1 = u(z_B)$ is the surface wind and $u_2 = u(-z_B)$ is the surface current (Fig. 1), and $K_I = ¼\,K(|z_B|)$ is the inertial drag coefficient, so named because the viscosities in air and water are not relevant in the analysis. Hence on transforming to the reference height in air, $z = 10$ m, assuming that a logarithmic profile occurs, we obtain,